Journal of Membrane Science and Research 7 (2021) 67-73

Journal of Membrane Science & Research

journal homepage: www.msrjournal.com

Research Paper

Effect of TiO_2 Nanoparticles on Barrier and Mechanical Properties of PVA Films

Maryam Zamanian [1], Hassan Sadrnia [1,*], Mehdi Khojastehpour [1], Fereshte Hosseini [2], Jules Thibault [3]

[1] *Department of Biosystems Engineering, Ferdowsi University of Mashhad, Iran*
[2] *Department of Food Additives, Iranian Academic Centre for Education Culture and Research (ACECR), Mashhad, Iran*
[3] *Department of Chemical and Biological Engineering, University of Ottawa, Ottawa, Ontario, Canada K1N 6N5*

Article info

Received 2019-08-19
Revised 2020-02-26
Accepted 2020-02-27
Available online 2020-02-27

Keywords

Nanocomposites
Poly(vinyl alcohol) (PVA)
Barrier property
Titanium oxide
Packaging

Graphical abstract

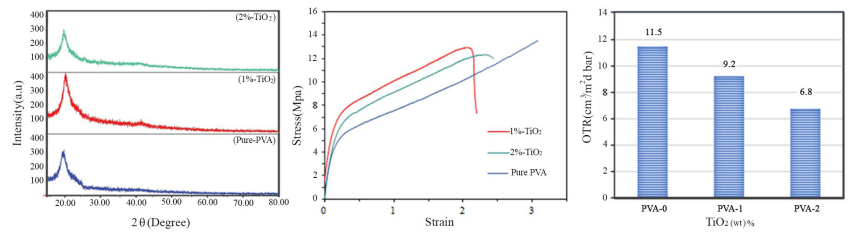

Highlights

- Effect of TiO_2 nanoparticle on the crystallinity of PVA matrix
- Oxygen transfer rate and water vapor permeability of nanocomposite films
- The morphology of nanocomposite films was examined via XRD and SEM
- Applying nano TiO_2 influenced the mechanical features

Abstract

Nanocomposites made of nanoparticles embedded in the matrix of polymer membranes have been used in the food packaging industry due to their enhanced barrier and mechanical properties. In this study, nanocomposite films made of polyvinyl alcohol (PVA) and titanium dioxide nanoparticles (size = 20 nm, 1 and 2 wt%) were prepared by the solvent casting method and their mechanical, physical, and barrier properties were determined. Scanning electron microscopy (SEM) and X-ray diffraction analysis (XRD) were performed for characterizing the morphology of PVA/TiO_2 nanocomposite films. Water vapor permeability (WVP) and oxygen transmission rate (OTR) were measured for mixed matrix PVA films for two concentrations of TiO_2 nanoparticles. The results revealed that OTR and WVP decreased with increasing TiO_2 nanoparticle concentration. Elongation at the break point and Young's modulus both increased whereas strength decreased. XRD measurements confirmed the completely dispersed structure formed in the TiO_2 nanocomposites. SEM micrographs showed an identical distribution at 1 and 2 wt% levels of TiO_2 nanoparticles.

1. Introduction

Food packaging creates and maintains suitable environmental conditions for preserving quality, ensuring safety, and increasing shelf life of food products by preventing aging and deterioration. Food packaging research, compared to other commodity packaging that is mainly used for damage protection, must address a much larger spectrum of concerns [1-3], as illustrated in Figure 1. Indeed, a myriad of factors such as deficiency, excess moisture and oxygen, the effect of light and temperature on food quality, packaging sustainability, and mechanical and physical properties to name only a few must be considered simultaneously in food packaging research. Food packaging has always been an active area of research in order to constantly improve packaging materials [4-6]. One area of research that has seen rapid development in the recent years is the use of mixed matrix membranes to enhance the properties of packaging materials such as improving barrier property by embedding impermeable particles in the polymer matrix or making use of the properties of membranes in novel ways to create modified atmosphere packaging and active packaging [7].

Polymer films have been used successfully for many years as barrier materials in food packaging. Barrier properties can be further enhanced by incorporating nanoparticles into the matrix of polymeric films [8,9]. Polyvinyl alcohol (PVA) as a good synthetic polymer has been widely used in various industries because of its water-solubility and great biocompatibility, compared to other barrier polymer films [10,11]. PVA has been adopted for numerous applications due to its good thermal stability, chemical resistance to oils, solvents and grease, and film-forming ability [12]. PVA has been used for instance for paper, textile and food supplement coating, adhesive and drug carrier. In addition to the above enviable characteristics, PVA has excellent physical properties (hardness, strength and flexibility) and it is nontoxic, biologically compatible and biodegradable [9,11,13,14]. Furthermore, the barrier properties of PVA toward oxygen, aroma and carbon dioxide have led to its effective application in food packaging [8,15]. On the negative side, PVA films are extremely sensitive to humidity, which has the effect of decreasing its stability and durability [16].

The physical and mechanical properties of polymer films, including PVA thin films, can be enhanced by various strategies like addition of nanofillers, copolymerization and blending. For the approach involving addition of nanofillers, carbon fibers, nanoclays, titanium oxide and many other nanoparticles have been used until now. They interact well with the polymer matrix, thereby favoring their physical binding with the surrounding polymer

* Corresponding author:E-mail address: hassan.sadrnia@um.ac.ir (H. Sadrnia)

DOI: 10.22079/JMSR.2020.112911.1283

and they significantly enhance some important polymer properties such as thermal, barrier and mechanical attributes due to nanofillers, high surface energy and large volumetric surface area [14,17-19].

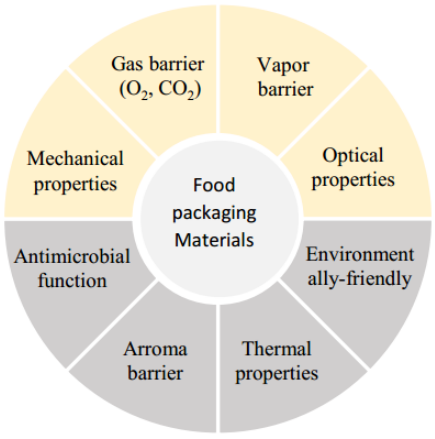

Fig. 1. Different purposes for food packaging material, Adapted from [5].

Among the many different types of nano-size fillers, TiO_2 nanoparticles have attracted significant research interest as nanofillers in polymeric films because of their good chemical stability, good refractive index at 600-nm wavelength (n = 2.38) [9], and their barrier and physicochemical properties [20-23]. In addition, titanium oxide nanoparticles are non-toxic, chemically inert, inexpensive, and resistant to corrosion and possess broadband UV filter properties. One additional enviable property is their anti-bacterial photo-irradiation effect [24]. Thin films formed by embedding TiO_2 nanoparticles within the polymer matrix display high chemo-mechanical permanence and can be used to provide protection against foodborne allergens and microorganisms in the presence of ultraviolet radiation [25]. The FDA approved TiO_2 as a "food contact substance" implying that it is safe to incorporate TiO_2 in polymeric barrier films for food packaging [26].

Improving barrier properties of packaging materials against oxygen diffusion and water vapor permeability is a major emphasis in food packaging and incorporation of inexpensive impermeable nanoparticles within the matrix of polymer films appears to be a viable research direction.

The objective of this study is to investigate the effects of incorporating relatively small amounts of TiO_2 nanoparticles in PVA-based thin films, with high molecular weight, on their structural, mechanical and especially barrier properties in comparison with previous studies [27,28]. It was desired to particularly examine whether or not accrued protection of oxygen and WVP-sensitive foods could be achieved, and if the nanoparticles would disperse effectively into the polymeric matrix to create tortuous diffusion pathways within the thin films to improve their barrier attributes.

2. Materials and methods

2.1. Materials

Polyvinyl alcohol (MW=145000 g/mole) was selected for improving the properties of food packaging films and comparing the literature results with those obtained with five different molecular weights i.e. 70000, 75000, 90000, 125000 and 145000 g/mole [29]. Polyvinyl alcohol (MW=145000 g/mole) and titanium oxide nanopowder (TiO_2, anatase, 99+%, and 20 nm according to the data sheet) used in this work have been purchased from Sigma–Aldrich Chemicals. The plasticizer, glycerol in this investigation, was purchased from Merck Co. (Germany).

2.2. Preparation of the films

The solution casting method was used to prepare PVA and PVA/TiO_2 nanocomposite films. First, for each sample, PVA (1.8 g) was dissolved in deionized water (50 mL) and maintained at room temperature for 24 h. The mixture was then brought to a temperature of 90˚C and blended with a magnetic stirrer up to 3 h to ensure that PVA was completely dissolved in water. The aqueous solution was chilled to room temperature. In parallel, various amounts of TiO_2 nanoparticles (1 & 2 wt% on a dry polymer basis) were added separately to deionized water (50 mL) and stirred for 12 h (500 rpm), followed by an agitation using an ultrasonic homogenizer for 20 min to ensure excellent particle dispersion. TiO_2 nanoparticle solution was then added to the PVA solution drop by drop under intense stirring (1000 rpm, 5 min). Finally, the plasticizer (30 wt% glycerol on a dry polymer basis) was added. To eliminate air bubbles from the solutions, vacuum was applied via a rotary vacuum pump. The solution was poured into a 15-cm internal diameter petri dish having a perfectly flat bottom and adjusted perfectly horizontally. Homogeneous films were obtained after drying in an air oven at 40˚C for 72 h.

2.3. Morphological analysis

The morphology of the cross-sectional area of specimen films was analyzed using a Scanning Electron Microscope (FE-SEM, TE-SCAN, MIRA3 Model) with an accelerating voltage of 5.0 kV. The cross sections of the barrier films were prepared by immersing the samples in liquid nitrogen and then breaking them, and finally coating the samples with gold.

2.4. X-ray diffraction analysis

X-ray diffraction (XRD) patterns for undoped and doped PVA films have been obtained using an X-ray diffraction spectrometer (Model Explorer, GNR Company, Italy) at 40 kV and 30 mA with a filtered 0.154 nm Cu K-α radiation. All tests were performed at ambient temperature in the reflection mode with 15˚ to 80˚ variation of 2θ.

2.5. Mechanical properties

The mechanical properties of each PVA film were determined using a Tensile Testing Machine (H5 KS, Manchester, U.K.). For each sample, three replicate measurements of tensile strength (TS), Young's modulus (YM), and elongation at the breakpoint (EB) were performed per ASTM Standard Method D882-02 (ASTM, 2002). Strain rate around 50 mm/min and distance of 5 cm were was selected for the two jaws of the Tensile Testing Machine [30].

2.6. Color and transparency

Barrier materials must have adequate optical transparency and proper color in order to meet industry standards. For measuring the color value of nanocomposite films, a colorimeter (Colorflex, USA) was used. Samples were evaluated for their amounts of red, green, and blue needed to form sample color, which provide lightness, chromaticity, and hue of the film sample. The information on color is based on International Commission on Illumination and is represented by a three-dimensional rectangular color space with parameters *L*, *a* and *b*. The parameter *L* is the lightness axis going from zero for black to 100 for white whereas the parameter *a* is the red to green axis with green in the negative side and red in the positive side, and finally the parameter *b* represents the blue to yellow axis with blue in the negative side and yellow in the positive side.

To evaluate the optical transparency of the films, light absorption at a wavelength of 600 nm was evaluated following the method proposed by Yan et al. [31] and using a UV-Vis spectrophotometer (CAMSPECM550 Model). Small rectangular samples were cut out of the barrier films for testing in the spectrometer and then their transparency was determined using Eq. 1 [32]:

$$Opacity = \frac{A_{600}}{d} \quad (1)$$

where A_{600} is the absorbance value at 600 nm and *d* represents the film thickness (mm).

2.7. Barrier properties

2.7.1. Water vapor permeability (WVP)

Two test methods are normally used for determination of water vapor transmission (WVT) of barrier films. The standard ASTM E96-95 test [33], namely the Desiccant Method, was followed in order to determine the WVP of barrier films in this investigation. The Desiccant Method with some modifications was performed in permeation cells having a mean diameter of 2 cm and a depth of 4.5 cm. Two grams of anhydrous potassium acetate were placed in each permeation cell and the cells were covered with specimens of barrier films with different combinations of TiO_2. Each permeation cell was put in a desiccator containing saturated NaCL solution in a small beaker at the bottom, resulting in a constant relative humidity (RH) of 75% at 25°C.

Permeation cells were weighed each 3 h over a 2-day period and water vapor transport was determined based on the weight increment of the permeation cell. WVP measurements were replicated three times. Water vapor permeation rate (WVP) was estimated from Eq. 2 [33]:

$$WVP = \frac{md}{At\Delta p} \quad \left[\frac{g}{mPa.s}\right] \tag{2}$$

where m is the mass gain of the cells over a given time period t, d is the average film thickness, A is the effective film area, and water vapor pressure difference is shown by Δp on both sides of the film, respectively.

2.7.2. Oxygen transmission rate

Oxygen transmission rate (OTR) of the barrier films was measured using a gas permeation instrument (Model D-80335 Brugger München Corporation, Germany) using pure oxygen at 25°C and 1 atm per ASTM D 3985 standard of [34]. Oxygen permeance is defined as the ratio of OTR to O_2 partial pressure difference between the two sides of the barrier films. The neat PVA films and the nanocomposite membranes, cast in a 15-cm internal diameter Petri dish, were all analyzed for OTR.

2.8. Contact angle measurements

Contact angles of nanocomposite films were determined using a contact angle meter (Static/Dynamic/High Temperature instrument, Iran) with the sessile drop method. A droplet of deionized water (4 µL) was carefully deposited on the top surface of the film and the dynamic contact angle was determined by fitting a mathematical equation to the water droplet shape and calculating the tangent between the water drop and solid film. Three replicates of contact angle measurements were performed for all samples.

3. Results and discussion

3.1. X-ray diffraction (XRD)

X-ray diffraction measurements were performed to examine the crystallinity of pure PVA and PVA/TiO_2 membranes. Figure 2 shows the XRD patterns of TiO_2 powder, pure PVA membranes and PVA/TiO_2 composite membranes with concentration of 1 and 2 wt% of TiO_2 nanoparticles. Figure 2a presents the XRD pattern of TiO_2 nanoparticles where characteristic diffraction peaks at 2θ = 26, 38, 37.65, 38.55, 48.7, 54, 63.08, 75.46, and 75.67° are revealed. The XRD pattern of TiO_2 powder shows an anatase characteristic structure. Figure 2b gives the XRD pattern of a pure PVA membrane showing an important diffraction peak located at 2θ = 19.37°. This peak is due to strong intermolecular and intramolecular hydrogen bonding [35] and it is indicative of a semi-crystalline structure. The characteristic peak for PVA agrees with the results reported by many authors including the work of Kim [36].

By combining a crystalline structure with distinct diffraction peaks found in titanium dioxide with a semi-crystalline polyvinyl alcohol structure, the resulting film also possesses a semi-crystalline structure as shown in Figure 2c. Although it is not readily obvious from Figure 2c due to the relatively low TiO_2 concentration, the XRD software showed peaks at 2θ = 19.96, 25.41, 36.94, 48.01 and 74.2°for PVA/1 wt% TiO_2 nanocomposite films, and peaks at 2θ = 20.08, 25.5, 38.22, 48.32, 55.38 and 63.08° for PVA/2 wt% TiO_2 nanocomposite films, which are indicative of the main PVA with the existence of embedded titanium dioxide.

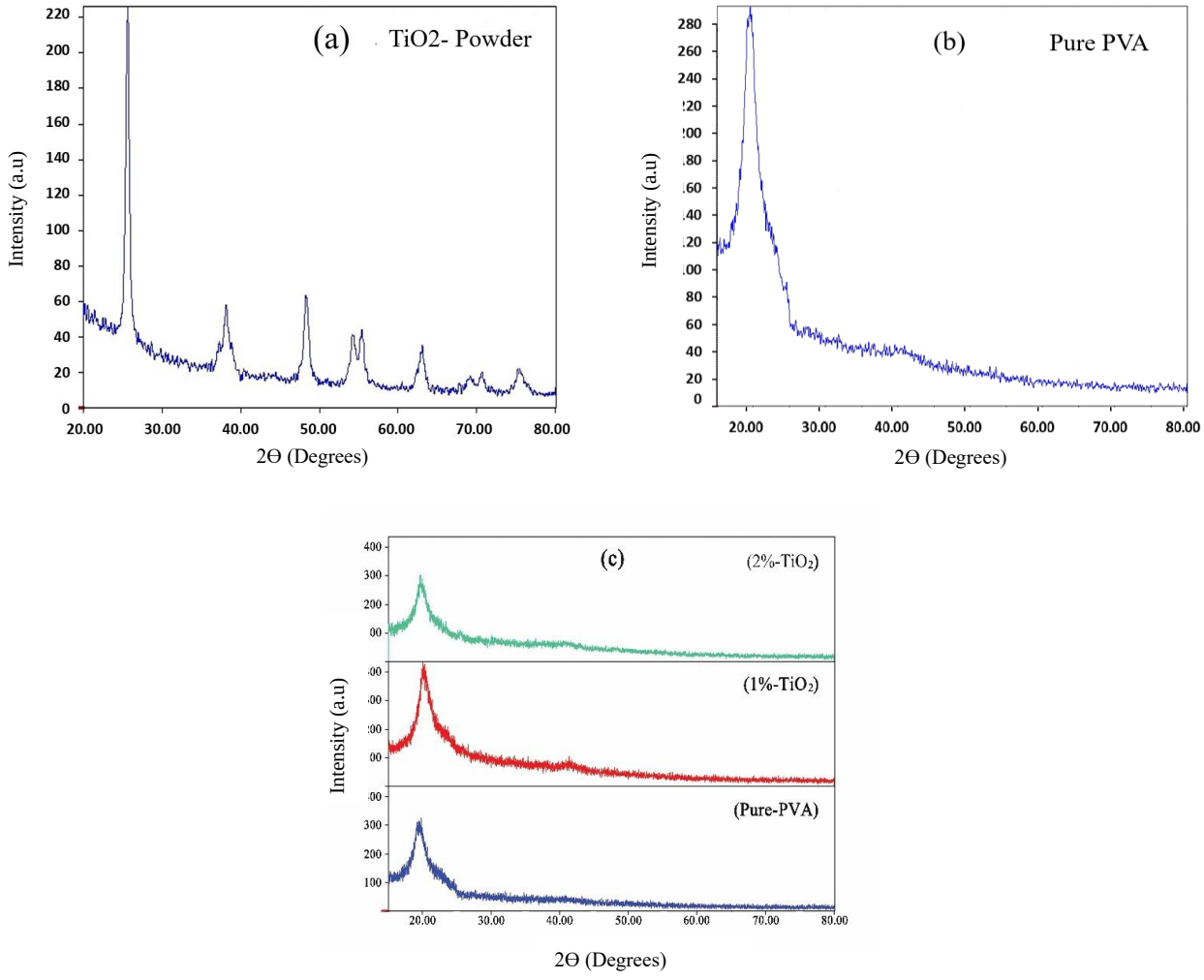

Fig. 2. XRD patterns of (a) TiO_2 powder, (b) Pure PVA membrane and (c) nanocomposite polymer films for three different concentrations (0, 1 and 2 wt%).

3.2. Morphological analysis

The morphology of cross sections for the specimen films was analyzed using SEM to study the distribution and dispersion of TiO_2 nanoparticles within the PVA nanocomposite films. SEM images of PVA loaded with 1 and 2 wt % TiO_2 are depicted in Figure 3. As it can be seen, evenly distributed TiO_2 nanoparticles are observed in the polymer matrix of the nanocomposite films. This is the reason why no prior treatment of nanoparticles was performed. In addition, the method for dispersing TiO_2 nanoparticles in PVA solution used in this investigation for the preparation of the nanocomposite films is appropriate.

3.3. Mechanical properties

The mechanical properties of all nanocomposite films were evaluated in order to assess film performance with respect to mechanical viability. Table 1 presents the values of elongation at breakpoint (EB), tensile strength (TS) and Young's Modulus (YM) for pure PVA and nanocomposite films. The stress–strain curves of PVA and PVA/TiO_2 nanocomposite films are presented in Figure 4. The results shown in Figure 4 and Table 1 show that the neat PVA membranes have the lowest YM value but the highest TS and EB values. It can be hypothesized that incorporation of TiO_2 within the matrix of the polymer limits the polymer chain movement of PVA because of the strong interplay between the nanoparticles and polymer matrix [37]. Moreover, it should be noted that TiO_2 nanofillers lead to a decrease in polymer network resistance against fractures [25]. Based on the results shown in Table 1, increase in nanoparticle loading in the polymer matrix leads to a decrease in percentage elongation at the breakpoint, which are similar to the results reported by Yun et al. [38]. Furthermore, Young's Modulus increased with an increase in the nanoparticle concentration as reported in the literature [39] even though some authors have shown inverse trends [13,27]. The results of this study show that there is a significant increase in the value of Young's Modulus for 1 wt% TiO_2 in PVA films, followed by a decrease for 2 wt% nanocomposite films. It appears that a particle loading of more than 1% TiO_2 leads to a reduction in resistance of the polymer network. It is possible that this decrease is associated with an increase in agglomeration of nanoparticles at a higher concentration such that a 1 wt% TiO_2 loading could be an optimum nanoparticle content for PVA nanocomposite films where a higher YM is desired. There are obviously many other parameters to consider and an optimum concentration would be the result of a compromise between many different thin film properties.

3.4. Color and opacity

Table 2 presents the three-color parameters (*L*, *a*, and *b*) of the three-dimensional rectangular color space, the whiteness index *WI* and the color difference ΔE relative to the standard plate parameters (*L**= 92.62, *a**= -1.24, *b**= 0.60) of neat PVA films and PVA/TiO_2 nanocomposite films. ΔE measures the color difference to a known set of coordinates and it is defined as the square root of the sum of squares of the differences between *L*, *a* and *b* values of the tested samples and their associated standard coordinates. To better assess the color difference due to addition of nanoparticles, ΔE was also calculated using the values of neat PVA membrane and it was reported for each sample in Table 2 in the second row element of the ΔE column.

The results of Table 2 show that all color values are impacted at different degrees with presence and amount of TiO_2 within the polymeric membrane. In general, all color parameters increased with an increase in TiO_2 filler content. However, before examining each of the color parameters, it important to mention that all films made in the laboratory have a very low opacity and the results must be analyzed considering the film as being very transparent, even though there is a small increase in opacity when nanoparticles are present.

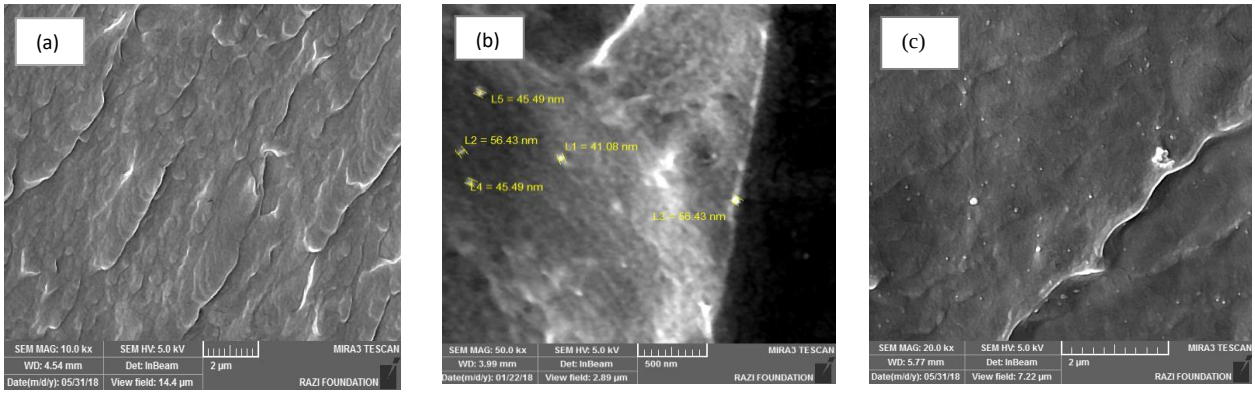

Fig. 3. SEM images of (a) 0 wt%, (b) 1 wt%, (c) 2 wt% PVA/TiO_2 nanocomposite films.

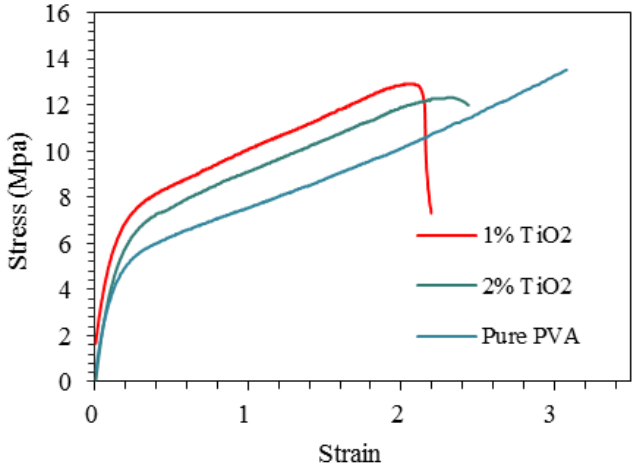

Fig. 4. Typical stress–strain plots for neat and nanocomposite films.

Table 1
Mechanical properties for neat and nanocomposite films.

Sample	Tensile Strength (MPa)	Young's modulus (MPa)	Elongation at break (%)
PVA-0	25.69±6.08	6.65±1.47	347.10±27.58
PVA-1	19.03±3.05	33.80±2.15	296.00±38.2
PVA-2	16.80±2.24	12.38±3.68	234.30±30.45

The color parameters of neat membranes are close to zero and it is considered to be black whereas when TiO_2 nanoparticles are incorporated within the PVA membrane it becomes whiter with L values in the vicinity of 40-45%. The parameter *a*, for the red to green axis, remains essentially constant near the value of zero. Parameter *b*, for the blue to yellow axis, tends to decrease slightly to the blue side of the axis. Overall, the color difference ΔE measured relative to neat PVA membrane shows a significant increase with nanoparticle concentration whereas ΔE values measured relative to the standard plate parameters decrease slightly. These results are generally in

agreement with the observations made by Goudarzi et al. [40] who stated that incorporation of TiO_2 nanoparticles in starch/TiO_2 bio-nanocomposite films led to increases in *L* and ΔE values whereas *a* and *b* were shown to decrease. In addition, Zolfi et al. [25] reported that in films of kefiran/whey protein embedding TiO_2 nanoparticles WI increased while ΔE decreased. The difference in the types of polymer, the crystallite type of TiO_2 nanoparticles, size of nanoparticles, the preparation method, and the membrane thickness are some of the reasons that led to different results in polymers and biopolymers.

PVA is a transparent material and presence of nanoparticles within the polymeric membranes leads to a reduction in its transparency. This is in agreement with the results usually presented in the literature [30] where it is reported that a decrease in transparency is observed when nanoparticles are incorporated within the polymer [41]. Transparency of PVA/1 wt% TiO_2 nanocomposite films was around 27%, which is close to the value reported by Wu et al. [27] for FK/PVA/Tris/TiO_2 nanocomposite films at 600 nm.

3.5. Barrier properties

3.5.1. Water Vapor Penetration (WVP)

WVP is an important parameter for biodegradable films used in the food packaging since it is desirable to minimize the moisture migration between food and the surrounding atmosphere. The results for water vapor penetration (WVP) for neat PVA and nanocomposite membranes with various loadings of TiO_2 nanoparticles are shown in Figure 5. Addition of TiO_2 nanoparticles in PVA membranes leads to a decrease in WVP and a larger reduction in penetration was observed at higher TiO_2 concentrations. The WVP of the nanocomposite film reaches a minimum of 0.89×10^{-10} $g^{-1}.Pa^{-1}.s^{-1}$ when the TiO_2 content is 2 wt%, which is 27 times less than the results reported by Wu et al. [27] who prepared FK/PVA/Tris/MMT/TiO_2 nanocomposite films using the solvent casting method. The reduction in water vapor penetration is due to the increase in tortuosity of the membrane. Since TiO_2 nanoparticles are non-porous and impermeable to migrating species, the diffusion path is further increased leading to a decrease in membrane permeability. In addition, inhibition of polymer chain movement also contributes to reduction in WVP. The results of this study agree with the results of previous studies. For example, increasing the amount of TiO_2 nanoparticles in the polymeric film led to a reduction in water vapor penetration of kefiran-whey protein isolate-TiO_2 films [25], CMC-MMT-TiO_2 films [42], and starch-TiO_2 films [28].

3.5.2. Oxygen transmission rate (OTR)

Oxygen transmission rate (OTR) was measured for neat PVA and nanocomposite membranes and the results are reported in Figure 6. The results show that addition of nanoparticles within the matrix of PVA increases the barrier properties of films with respect to permeation of oxygen. According to ASTM D-3985, oxygen permeability experiments were performed under constant feed pressure. OTR of the nanocomposite films decreased, respectively, by 20% and 41% for 1 wt% and 2 wt% TiO_2 nanoparticles in comparison with the pure PVA films as shown in Figure 6.

The presence of nanoparticles in the polymeric matrix offers an additional physical barrier to permeation of oxygen through the membranes. It is hypothesized that this decrease is mainly due to the restriction in movement of polymer chains by the nanoparticles and to the more tortuous path that oxygen molecules must take to go around the non-porous nanofillers. Similar results for the reduction of the transmission rate of gases were reported previously for PBAT/TiO_2 nanocomposite thin films [43] and LDPE/TiO_2 films [44]. Also in comparison with the results reported by Wu et al. [27], the OTR measured in this study show a reduction in value by around 22.73% at 2 wt% TiO_2.

An additional reason for the decrease in OTR is the changes to the polymer matrix occurring at the interfacial regions due to the presence of TiO_2 nanoparticles [45].

Table 2
Assessment of color and opacity of various different PVA/TiO_2 nanocomposites.

Sample	Thickness (mm)	L^*	a^{**}	b^{***}	ΔE^{****}	WI^{*****}	Opacity (%)
PVA-0	0.11±0.03	2.89±0.21	0.18±0.13	-0.54±0.04	89.75±0.21 0.00±0.28	2.88±0.21	0.45±0.10
PVA-1	0.11±0.04	38.67±1.33	0.18±0.04	-10.99±0.08	55.20±1.29 61.97±1.33	37.69±1.30	3.65±1.39
PVA-2	0.15±0.01	46.44±2.41	0.67±0.24	-15.21±0.73	48.86±2.08 75.43±2.53	44.30±2.14	3.11±0.08

* Lightness index
** Red to green index
*** Blue to yellow index
**** Color difference index
***** Whiteness index

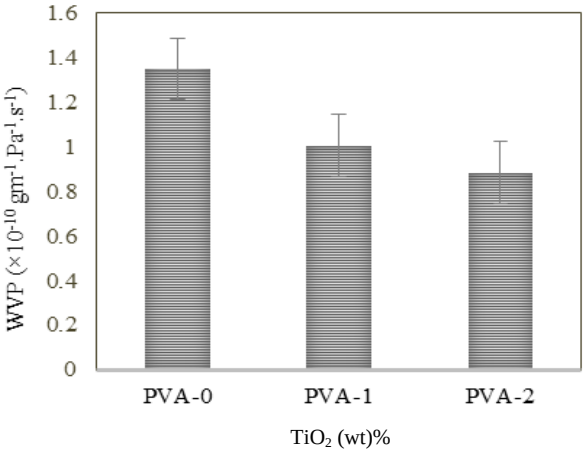

Fig. 5. WVP for neat PVA membrane and PVA/TiO_2 nanocomposite films.

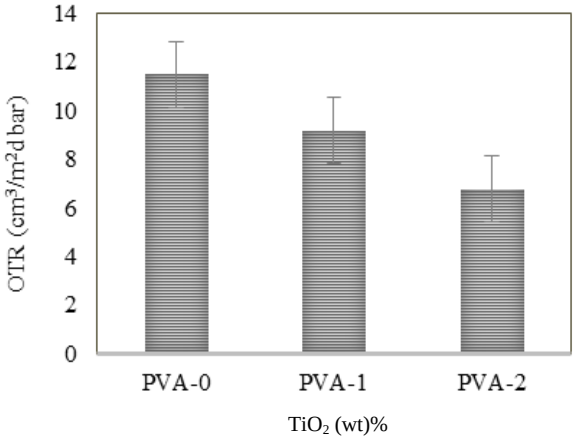

Fig. 6. Oxygen transmission rate of neat PVA membrane and nanocomposite films measured at 25˚C and with a feed pressure of 1 atm.

3.6. Contact angle measurements

The surface hydrophobicity of nanocomposite films is an important factor that can affect permeation flux through thin films. It was evaluated via contact angle measurements and the results are presented in Figure 7 for different nanoparticle contents. The initial contact angle of neat PVA film was 51.1˚. By addition of 1 and 2 wt% TiO_2 nanoparticles, the contact angle increased to 53.3˚ and 66.9˚, respectively which demonstrate that addition of TiO_2 nanoparticles can increase hydrophobicity of neat PVA films. In fact, incorporation of nanoparticles affects the roughness of film surface, and a rougher structure of the film surface is one of the main reasons for increase of hydrophobicity [46]. Although our results are in contrast to those reported by Ahmad et al. [47] for PVA films reinforced with high content of TiO_2, these results confirm reduction of water vapor penetration when TiO_2 nanoparticles are embedded into neat PVA films. Hence, these nanocomposite films are good candidates for food packaging. In addition, contact angle images of different types of nanocomposite films are presented in Figure 8.

4. Conclusions

Neat PVA films and PVA films embedding TiO_2 nanoparticles were successfully prepared by the solution and casting methods. Their properties were investigated from a structure point of view and morphology of the films. The results clearly indicate that TiO_2 nanoparticles are embedded uniformly within the PVA matrix. XRD analysis showed that TiO_2 nanoparticles were indeed incorporated within the PVA polymer matrix and crystallinity was strongly influenced by the amount of TiO_2 nanoparticles present. In addition, it was seen that by incorporation of TiO_2 nanoparticles into the PVA matrix to form a thin composite film, the mechanical properties of nanocomposites were partly changed. A decrease in transparency and an increase in whiteness were observed. Incorporating nanoparticles into the PVA matrix led to a decrease in WVP and OTR, thereby resulting in enhancement of the barrier properties of nanocomposite films. The observed increase in surface hydrophobicity of nanocomposite films confirmed the WVP. PVA films with 2 wt% TiO_2 showed maximum improvement in oxygen barrier properties with a 41% reduction in OTR. However, the resistance to water and mechanical and barrier properties of neat PVA were improved significantly by adding nanoparticles. Additional studies are needed to determine under which conditions nanocomposites can be used the best, and to develop methods to overcome limitations of these polymeric films under wet conditions.

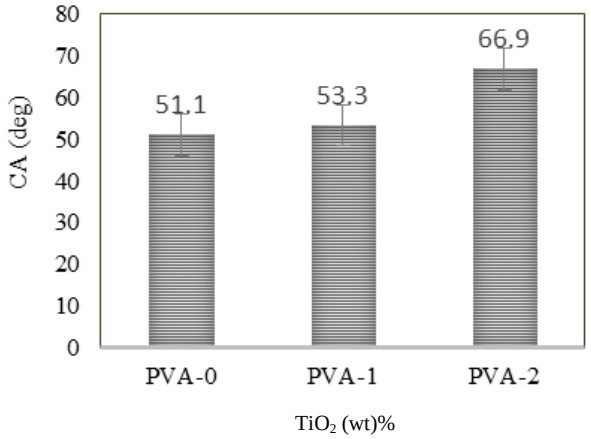

Fig. 7. Effect of TiO_2 on the contact angle of TiO_2/PVA nanocomposite films.

Acknowledgments

The authors gratefully acknowledge the financial support provided by the Ferdowsi University of Mashhad (Grant No. 44023). The authors declare that they have no conflict of interest.

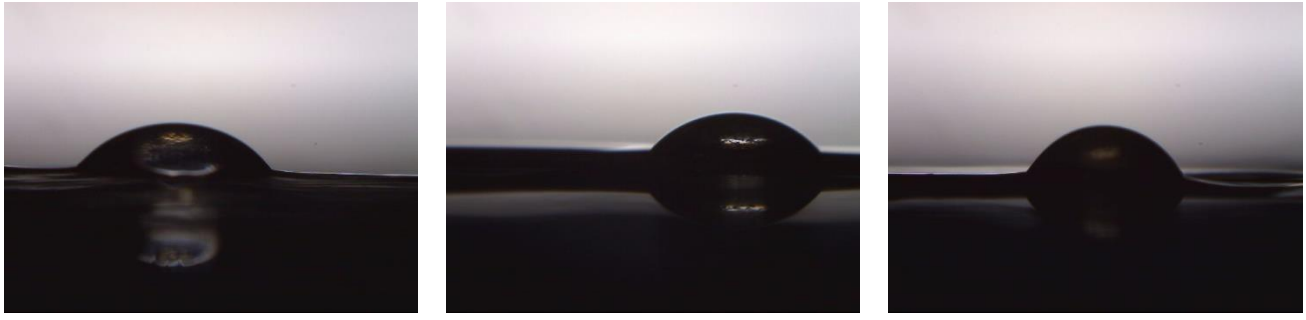

Fig. 8. Contact angle images of (a) neat PVA, (b) 1% TiO_2/PVA, (c) 2% TiO_2/PVA nanocomposites.

References

[1] R.P. Singh, B. Anderson, The major types of food spoilage: an overview, in: R. Steele (Ed.), Understanding and measuring the shelf-life of food, 2004, pp. 3-23.
[2] G.D.L.E. Mauriello, E. De Luca, A. La Storia, F. Villani, D. Ercolini, Antimicrobial activity of a nisin-activated plastic film for food packaging, Lett. Appl. Microbiol. 41 (2005) 464-469. DOI: 10.1111/j.1472-765X.2005.01796.x.
[3] H. Brown, J. Williams, M. Kirwan, Packaged Product Quality and Shelf Life, in: R. Coles, M.J. Kirwan (Eds.), Food and Beverage Packaging Technology, 2011, pp. 59-83.
[4] E. Bakkalbaşı, Ö.M. Yılmaz, I. Javidipour, N. Artık, Effects of packaging materials, storage conditions and variety on oxidative stability of shelled walnuts, LWT-Food Sci. Technol. 46 (2012) 203-209. DOI: 10.1016/j.lwt.2011.10.006.
[5] J.W. Rhim, H.M. Park, C.S. Ha, Bio-nanocomposites for food packaging applications, Prog. polym. Sci. 38 (2013) 1629-1652. DOI: 10.1016/j.progpolymsci.2013.05.008.
[6] N.E. Kochkina, O.A. Butikova, Effect of fibrous TiO_2 filler on the structural, mechanical, barrier and optical characteristics of biodegradable maize starch/PVA composite films, Int. J. Biol. Macromol. 139 (2019) 431-439. DOI: 10.1016/j.ijbiomac.2019.07.213.
[7] A. Figoli, E. Mascheroni, S. Limbo, E. Drioli, Membranes for Food Packaging, Membrane Technology, 3 2010. DOI: 10.1007/978-3-662-44324-8_851.
[8] S.E. Selke, J.D. Culter, Plastics packaging: properties, processing, applications, and regulations, Carl Hanser Verlag GmbH Co KG, 2016.
[9] V. Kaler, U. Pandel, R. Duchaniya, Development of TiO_2/PVA nanocomposites for application in solar cells, Mater. Today, Proceedings, 5 (2018) 6279-6287. DOI: 10.1016/j.matpr.2017.12.237.
[10] J.Y. Woo, E.J. Shin, Y.H. Lee, Effect of boric acid treatment on the crystallinity and drawability of poly (vinyl alcohol)–iodine complex films, Polym. Bull. 65 (2010) 169-180. DOI: 10.1007/s00289-010-0279-9.
[11] S. Muppalaneni, H. Omidian, Polyvinyl alcohol in medicine and pharmacy, a perspective, J. Develop. Drug. 2 (2013) 1-5. DOI: 10.4172/2329-6631.1000112. DOI: 10.4172/2329-6631.1000112.
[12] O.W. Guirguis, M.T. Moselhey, Thermal and structural studies of poly (vinyl alcohol) and hydroxypropyl cellulose blends, Nat. Sci. 4 (2012) 57. DOI: 10.4236/ns.2012.41009.
[13] M.I. Baker, S.P. Walsh, Z. Schwartz, B.D. Boyan, A review of polyvinyl alcohol and its uses in cartilage and orthopedic applications, J. Biomed. Mater. Res. B Appl. Biomater. 100 (2012) 1451-1457. DOI: 10.1002/jbm.b.32694.
[14] J. Ding, C. Zhao, L. Zhao, Y. Li, , D. Xiang, Synergistic effect of α-ZrP and graphene oxide nanofillers on the gas barrier properties of PVA films. J. Appl. Polym. Sci. 135 (2018) 46455. DOI: 10.1002/app.46455.

[15] H.A. Silvério, W.P.F. Neto, D. Pasquini, Effect of incorporating cellulose nanocrystals from corncob on the tensile, thermal and barrier properties of poly (vinyl alcohol) nanocomposites, J. Nanomater. (2013) 74. DOI: 10.1155/2013/289641.
[16] J.H. Jang, J.I. Han, Cylindrical relative humidity sensor based on poly-vinyl alcohol (PVA) for wearable computing devices with enhanced sensitivity, Sensor. Actuat. A Phys. 261 (2017) 268-273. DOI: 10.1016/j.sna.2017.05.011.
[17] B. Ghanbarzadeh, S.A. Oleyaei, H. Almasi, Nanostructured materials utilized in biopolymer-based plastics for food packaging applications, Crit. Rev. Food Sci. Nutrit. 55 (2015) 1699-1723. DOI: 10.1080/10408398.2012.731023.
[18] G. Choudalakis, A. Gotsis, Permeability of polymer/clay nanocomposites: a review, Eur. Polym. J. 45 (2009) 967-984. DOI: 10.1016/j.eurpolymj.2009.01.027.
[19] M.J. Khalaj, H. Ahmadi, R. Lesankhosh, G. Khalaj, Study of physical and mechanical properties of polypropylene nanocomposites for food packaging application: Nano-clay modified with iron nanoparticles, Trend. Food Sci. Technol. 51 (2016) 41-48. DOI: 10.1016/j.tifs.2016.03.007.
[20] N.A. Ali, F.T.M. Noori, Gas barrier properties of biodegradable polymer nanocomposites films, Chem. Mater. Res. 6 (2014).
[21] J. Ren, S. Wang, C. Gao, X. Chen, W. Li, F. Peng, TiO_2-containing PVA/xylan composite films with enhanced mechanical properties, high hydrophobicity and UV shielding performance, Cellulose 22 (2015) 593-602. DOI: 10.1007/s10570-014-0482-1.
[22] M. Farhoodi, M. Mousavi, G.R. Sotudeh, D.Z. Emam, A. Oromiehie, Effect of TiO_2 nanoparticles on mechanical and transport properties of polyethylene terephthalate (pet) packages, 2017.
[23] N. Nakayama, T. Hayashi, Preparation and characterization of poly (L-lactic acid)/TiO_2 nanoparticle nanocomposite films with high transparency and efficient photodegradability, Polym. Degrad. Stab. 92 (2007) 1255-1264. DOI: 10.1016/j.polymdegradstab.2007.03.026.
[24] L.T. Lim, R. Auras, M. Rubino, Processing technologies for poly (lactic acid). Prog. polym. Sci. 33 (2008) 820-852. DOI: 10.1016/j.progpolymsci.2008.05.004.
[25] M. Zolfi, F. Khodaiyan, M. Mousavi, M. Hashemi, Development and characterization of the kefiran-whey protein isolate-TiO_2 nanocomposite films, Int. J. Biolog. Macromol. 65 (2014) 340-345. DOI: 10.1016/j.ijbiomac.2014.01.010.
[26] A. Martirosyan, Y.J. Schneider, Engineered nanomaterials in food: implications for food safety and consumer health, Int. J. Environ. Res. Pub. Health 11 (2014) 5720-5750. DOI: 10.3390/ijerph110605720.
[27] S. Wu, X. Chen, M. Yi, J. Ge, G. Yin, X. Li, M. He, Improving Thermal, Mechanical, and Barrier Properties of Feather Keratin/Polyvinyl Alcohol/Tris (hydroxymethyl) aminomethane Nanocomposite Films by Incorporating Sodium Montmorillonite and TiO_2. Nanomaterials 9 (2019) 298. DOI: 10.3390/nano9020298.
[28] S.A. Oleyaei, Y. Zahedi, B. Ghanbarzadeh, A.A. Moayedi, Modification of physicochemical and thermal properties of starch films by incorporation of TiO_2 nanoparticles, Int. J. Biolog. Macromol. 89 (2016) 256-264. DOI: 10.1016/j.ijbiomac.2016.04.078.
[29] F.L. Marten, Vinyl Alcohol Polymers. Encyclopedia of Polymer Science and Technology. 2002, John Wiley & Sons, Inc., USA. DOI: 10.1002/0471238961.2209142513011820.a01.
[30] E. Gharoy Ahangar, M.H. Abbaspour-Fard, N. Shahtahmassebi, M. Khojastehpour, P. Maddahi, Preparation and characterization of PVA/ZnO nanocomposite, J. Food Proc. Preserv. 39 (2015) 1442-1451. DOI: 10.1111/jfpp.12363.
[31] Q. Yan, H. Hou, P. Guo, H. Dong, Effects of extrusion and glycerol content on properties of oxidized and acetylated corn starch-based films, Carb. Polym. 87 (2012) 707-712. DOI: 10.1016/j.carbpol.2011.08.048.
[32] J.H. Han, J.D. Floros, Casting antimicrobial packaging films and measuring their physical properties and antimicrobial activity, J. Plastic Film Sheet. 13 (1997) 287-298. DOI: 10.1177/875608799701300405.
[33] A. Standard, Annual book of ASTM standards. American Society for Testing and Materials Annual, Philadelphia, PA, USA, 4 (2004).
[34] A. International, ASTM Standards: Standards Test Methods and Definitions for Mechanical Testing of Steel Products (A370-02), ASTM (2005).
[35] A. El-Shamy, W. Attia, K.A. El-Kader, The optical and mechanical properties of PVA-Ag nanocomposite films, J. Alloy. Comp., 590 (2014) 309-312. DOI: 10.1016/j.jallcom.2013.11.203.
[36] S.W. Kim, Preparation and barrier property of poly (vinyl alcohol)/SiO_2 hybrid coating films, Korean J. Chem. Eng. 25 (2008) 1195-1200. DOI: 10.1007/s11814-008-0197-9.
[37] X. Cao, Y. Chen, P.R. Chang, M. Stumborg, M.A. Huneault, Green composites reinforced with hemp nanocrystals in plasticized starch, J. Appl. Polym. Sci. 109 (2008) 3804-3810. DOI: 10.1002/app.28418.
[38] Y.H. Yun, Y.N. Youn, S.D. Yoon, J.U. Lee, Preparation and physical properties of starch-based nanocomposite films with the addition of titanium oxide nanoparticles, J. Ceram. Proc. Res. 13 (2012) 59-64.
[39] M.S. Islam, R. Masoodi, H. Rostami, The effect of nanoparticles percentage on mechanical behavior of silica-epoxy nanocomposites, J. Nanosci. (2013). DOI: 10.1155/2013/275037.
[40] V. Goudarzi, I. Shahabi-Ghahfarrokhi, A. Babaei-Ghazvini, Preparation of ecofriendly UV-protective food packaging material by starch/TiO_2 bio-nanocomposite: Characterization, Int. J. Biolog. Macromol. 95 (2017) 306-313. DOI: 10.1016/j.ijbiomac.2016.11.065.
[41] M. Abdollahi, M. Rezaei, G. Farzi, A novel active bionanocomposite film incorporating rosemary essential oil and nanoclay into chitosan, J. Food Eng. 111 (2012) 343-350. DOI: 10.1016/j.jfoodeng.2012.02.012.
[42] B.F. Achachlouei, Y. Zahedi, Fabrication and characterization of CMC-based nanocomposites reinforced with sodium montmorillonite and TiO_2 nanomaterials, Carbo. Polym. 199 (2018) 415-425. DOI: 10.1016/j.carbpol.2018.07.031.
[43] R. Venkatesan, N. Rajeswari, TiO_2 nanoparticles/poly (butylene adipate-co-terephthalate) bionanocomposite films for packaging applications, Polym. Adv. Technol. 28 (2017) 1699-1706. DOI: 10.1002/pat.4042.
[44] A. Nasiri, M. Shariaty-Niasar, Z. Akbari, Synthesis of LDPE/Nano TiO_2 nanocomposite for packaging applications, Int. J. Nanosci. Nanotechnol. 8 (2012) 165-170.
[45] A. Bhatia, R.K. Gupta, S.N. Bhattacharya, H.J. Choi, Analysis of gas permeability characteristics of poly (lactic acid)/poly (butylene succinate) nanocomposites, J. Nanomater. 6 (2012). DOI: 10.1155/2012/249094.
[46] X. Hou, P.T. Deem, K.-L. Choy, Hydrophobicity study of polytetrafluoroethylene nanocomposite films, Thin Solid Film. 520 (2012) 4916-4920. DOI: 10.1016/j.tsf.2012.02.074.
[47] J. Ahmad, K. Deshmukh, M. Habib, M.B. Hägg, Influence of TiO_2 nanoparticles on the morphological, thermal and solution properties of PVA/TiO_2 nanocomposite membranes. Arabian J. Sci. Eng. 2014. 39(10): p. 6805-6814. DOI: 10.1007/s13369-014-1287-0.